OPTOELECTRONICS LETTERS Vol.18 No.10, 15 October 2022

SER performance investigation of UWOC system over composite EGG oceanic turbulence fading channel with BSF*

YANG Pengfei, PANG Weina, LI Shuang, WANG Ping, CHEN Wenwen, and CHE Hui**
State Key Laboratory of Integrated Service Networks, School of Telecommunications Engineering, Xidian University, Xi'an 710071, China

(Received 26 February 2022; Revised 23 May 2022)

In this work, the symbol error rate (*SER*) performance of a relay-assisted underwater wireless optical communication (UWOC) system has been investigated over the composite exponential-generalized gamma (EGG) distribution with the beam spread function (BSF) under two hard decision schemes of fixed decision threshold (FDT) and dynamic decision threshold (DDT). Specifically, the oceanic turbulence is assumed to follow the EGG distribution, and the impacts of absorption, scattering and misalignment loss are characterized by BSF. The cumulative distribution function (CDF) of this UWOC system is derived with the max-min criterion as the best path selection scheme. And with the help of Gauss-Laguerre quadrature function, the analytical *SER* expressions for these two threshold schemes are then achieved and validated by Monte Carlo (MC) simulation. Moreover, the *SER* performance is further studied under different temperature gradients, bubble levels (*BLs*) and water salinity over three water types, as well as the system structure parameters. Results show that the UWOC system with DDT scheme can efficiently overcome the error floor induced by FDT scheme and demonstrates better *SER* performance. Furthermore, the *SER* performance would be improved with lower *BL*, temperature gradients and water salinity as well as the concentration of dissolved particles. This work will benefit the design and research of relay-assisted UWOC system.
Document code: A **Article ID:** 1673-1905(2022)10-0606-7
DOI https://doi.org/10.1007/s11801-022-2031-8

Underwater wireless optical communication (UWOC) is one of the emerging techniques for the realization of exploiting, discovering and protecting various underwater resources[1]. And the UWOC system has received considerable attention for the years due to its advantages of higher transmission security, higher data rates, lower latency and lower energy consumption[2,3]. Nevertheless, there are still some challenges in the UWOC technology. For instance, the performance of UWOC system would be severely degraded by the effects of absorption and scattering caused by the UWOC channel, and underwater optical turbulence (UOT) results from intensity fluctuations in the refractive index of seawater introduced by salinity variations, temperature variations as well as the presence of air bubbles[4,5].

To comprehensively study the statistics of intensity fluctuations in underwater channel with air bubbles, random temperature and salinity, a unified and more generalized UWOC turbulence model, the mixture exponential-generalized gamma (EGG) distribution has been proposed recently[6,7]. It provides outstanding goodness of fit for the given channel conditions through the further investigation of its measured data from weak to strong turbulence condition[8]. Furthermore, the misalignment loss in UWOC system is also one undesired effect due to the inducement of temporal communication interruptions and the degradation of the system performance[9]. And in the UWOC system, the impact of absorption, scattering and misalignment loss could be modeled by beam spread function (BSF)[9,10].

The structure of multi-hop relay-assisted transmission is a superior candidate to strengthen the connectivity of network and expand the communication range[3,11]. In addition, modulation scheme also plays a great role in communication systems. The multipulse pulse position modulation (MPPM) can improve band-utilization efficiency and has higher optical power utilization than the pulse position modulation and the on-off-keying modulation[12]. Moreover, the decision scheme at receiver also has significant impact on the transmission quality and system performance, which normally includes two important decision techniques, soft decision and hard decision. Compared with soft decision, the hard decision technique can efficiently degrade the sensitivity of time error and implementation complexity[13]. Nevertheless, to the best of our knowledge, the symbol error rate (*SER*) performance analysis of an MPPM UWOC system with hard decision schemes over the EGG distributed fading

* This work has been supported by the Key Research and Development Program of Shaanxi Province (No.2022GY-103) and the National Natural Science Foundation of China (No.62071365).
** E-mail: pingwang@xidian.edu.cn

channels combining the impact of absorption, scattering and misalignment has never been reported up to now.

In this work, employing the MPPM scheme, a multi-hop parallel UWOC system has been studied with two hard decision schemes over the combined EGG oceanic turbulence distribution including the impact of absorption, scattering, and misalignment loss described by BSF. With the max-min criterion as the best path selection scheme, the analytical *SER* expressions of this UWOC system over these two decision schemes are derived with the help of Gauss-Laguerre quadrature rule. Moreover, the proposed *SER* model is verified by Monte Carle (MC) simulation.

Fig.1 shows a multi-hop parallel UWOC communication system. Between the source and destination nodes, a direct link and R cooperative paths with $C-1$ relay nodes in each cooperative path are assumed. Considering the intensity-modulation and direct-detection (IM/DD) and (Q, P) MPPM scheme, where Q and P represent the numbers of time slots and pulses in one block respectively, the received signal at the jth hop in the ith path can be denoted as

$$y_{i,j}=R_{\mathrm{P}}h_{i,j}P_{i,j}x_{i,j}+n_{i,j}, \tag{1}$$

where R_{P} is the photodetector responsivity, $h_{i,j}$ is the aggregated channel gain at the jth hop in the ith path, $P_{i,j}$ represents the average transmitted optical power in each link, $x_{i,j}$ represents the input MPPM signal, and $n_{i,j}$ is the additive white Gaussian noise (AWGN) with zero mean and a variance of $\sigma_n^2=N_0/2$.

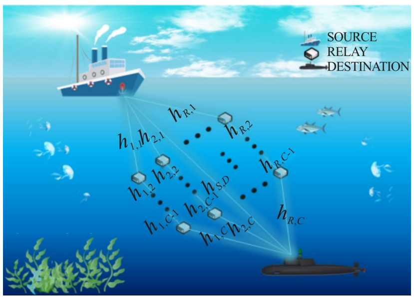

Fig.1 Multi-hop parallel UWOC system

Considering the air bubbles and temperature-induced irradiance fluctuations in both fresh and salty waters, the received light irradiance I is a weighted sum of exponential and generalized gamma distribution, which is given in Refs.[6] and [7] as

$$f_{\mathrm{EGG}}(I)=\varpi f\left(I;\lambda_{\mathrm{EGG}}\right)+\\ (1-\varpi)g\left(I;\left[a_{\mathrm{EGG}},b_{\mathrm{EGG}},c_{\mathrm{EGG}}\right]\right), \tag{2}$$

where f and g are the exponential and generalized gamma distributions, respectively, λ_{EGG} is the parameter of the exponential distribution, a_{EGG}, b_{EGG} and c_{EGG} are the parameters of the generalized gamma distribution, and ϖ is the mixture weight of these two distributions, satisfying $0<\varpi<1$. $\Gamma(x)=\int_0 t^{x-1}e^{-t}\mathrm{d}t$ represents the gamma function. Thus, the probability density function (PDF) of the oceanic turbulence-induced fading h_{a} can be expressed as[14,15]

$$f_{\mathrm{EGG}}\left(h_{\mathrm{a}}\right)=\frac{\varpi}{\lambda_{\mathrm{EGG}}}\exp\left(-\frac{h_{\mathrm{a}}}{\lambda_{\mathrm{EGG}}}\right)+(1-\varpi)\times\\ \frac{c_{\mathrm{EGG}}h_{\mathrm{a}}^{a_{\mathrm{EGG}}c_{\mathrm{EGG}}-1}}{\Gamma\left(a_{\mathrm{EGG}}\right)b_{\mathrm{EGG}}^{a_{\mathrm{EGG}}c_{\mathrm{EGG}}}}\exp\left(-\left(\frac{h_{\mathrm{a}}}{b_{\mathrm{EGG}}}\right)^{c_{\mathrm{EGG}}}\right). \tag{3}$$

Considering the effect of misalignment, the path loss h_{l} is characterized by the BSF, which can be expressed in Refs.[9] and [10] as

$$\mathrm{BSF}(Z_{\mathrm{rec}},r)=E_0(Z_{\mathrm{rec}},r)\exp(-cZ_{\mathrm{rec}})+\\ \frac{1}{2\pi}\int_0^{\infty}E_0(Z_{\mathrm{rec}},v)\exp(-cZ_{\mathrm{rec}})\times\\ \left[\exp\left(\int_0^{Z_{\mathrm{rec}}}b\tilde{\beta}(v(Z_{\mathrm{rec}}-z))\mathrm{d}z\right)-1\right]J_0(vr)v\mathrm{d}v, \tag{4}$$

where Z_{rec} is the link length between the source and receiver points, and r denotes the distance of the receiver aperture center from the beam center on the receiver plane. $E_0(Z_{\mathrm{rec}}, v)$ and $E_0(Z_{\mathrm{rec}}, r)$ are the irradiance distributions of the laser source in the spatial frequency domain and the spatial coordinate system, respectively. $\tilde{\beta}(v(Z_{\mathrm{rec}}-z))$ is the Hankel transform of the scattering phase function (SPF), and $J_0(vr)$ is the Bessel function. $a(\lambda)$, $b(\lambda)$ and $c(\lambda)$ are the absorption, scattering and extinction coefficients respectively, satisfying $c(\lambda)=a(\lambda)+b(\lambda)$. In addition, the values of typical coefficient for three underwater environments have been shown in Tab.1. With the help of Ref.[9], $h_{\mathrm{l}}=\mathrm{BSF}/P_{\mathrm{int}}$ can be obtained, in which P_{int} is the function of input power.

Tab.1 Coefficient values of various water types

Water type	a (m^{-1})	b (m^{-1})	c (m^{-1})
Pure sea water	0.040 5	0.002 5	0.043
Clean ocean	0.114 0	0.037 0	0.151
Coastal ocean	0.179 0	0.219 0	0.398

Thus, considering the ocean turbulence-induced fading h_{a} and the path loss h_{l}, the aggregated channel gain can be expressed as $h=h_{\mathrm{a}}h_{\mathrm{l}}$, and the CDF of h for the aggregated channel gain of UWOC system can be derived as

$$F_h(h)=\varpi-\varpi\exp\left(-\frac{h}{\lambda_{\mathrm{EGG}}h_{\mathrm{l}}}\right)+\\ \frac{1-\varpi}{\Gamma\left(a_{\mathrm{EGG}}\right)}\gamma\left(a_{\mathrm{EGG}},\left(\frac{h}{b_{\mathrm{EGG}}h_{\mathrm{l}}}\right)^{c_{\mathrm{EGG}}}\right). \tag{5}$$

Based on the multi-hop parallel architecture, the max-min criterion is adopted as the best path section scheme. The maximal instantaneous signal-to-noise ratio (*SNR*) is selected as the approximate end-to-end (EE) *SNR* at the destination, thus the below result can be got[16]

$$\gamma_{\max}=\max\left(\max_{i=1,\cdots,R}\left(\min_{j=1,\cdots,C}\left(\gamma_{i,j}\right)\right),\gamma_{\mathrm{s,d}}\right), \tag{6}$$

where $\gamma_{\mathrm{s,d}}$ and $\gamma_{i,j}$ represent the instantaneous *SNR* of the direct link from the source to destination and the instantaneous *SNR* at the jth hop in the ith path, respectively. Assuming that the channels are identically and independent distributed (i.i.d.) and all the hops have the same average *SNR* including the direct link, the CDF of *h* for the multi-hop parallel UWCO system can be expressed as

$$F_{\mathrm{M}}(h)=\left(1-\left[1-F_{h_{i,j}}(h)\right]^{C}\right)^{R}\times F_{h_{\mathrm{s,d}}}(h), \tag{7}$$

where $F_{h_{\mathrm{s,d}}}(h)$ is the CDF of the direct link from the source to destination, and $F_{h_{i,j}}(h)$ represents the CDF of the aggregated channel gain *h* of the *j*th hop in the *i*th path. Considering the i.i.d. links, the CDF of *h* for the multi-hop parallel UWOC system can be finally derived as $F_{\mathrm{M}}(h)=\left(1-\left[1-F_h(h)\right]^{C}\right)^{R}\times F_h(h)$.

For (*Q*, *P*) MPPM, considering the received signal is detected slot by slot, the output of the sampler can be expressed as

$$y=\begin{cases}\mu h+n & \text{signal time slot}\\ n & \text{non-signal time slot}\end{cases}, \tag{8}$$

where $\mu=QP_0R_p/P$. When the signal time slot or the non-signal time slot is transmitted, since the variables *h* and *n* are independent, the PDF of the sampled signal can be denoted as

$$f\left(y|\,y_0\right)=f_n(y)=\frac{1}{\sqrt{2\pi}\sigma_n}\exp\left(-\frac{y^2}{2\sigma_n^2}\right), \tag{9}$$

$$f\left(y|\,y_1\right)=\frac{1}{\mu}f_{\mathrm{M}}\left(\frac{y}{\mu}\right)\otimes f_n(y)=$$
$$\frac{1}{\sqrt{2\pi}\mu\sigma_n}\int_0^\infty\exp\left(-\frac{(y-s)^2}{2\sigma_n^2}\right)\times$$
$$\left(\begin{array}{l}RC\left(1-\left[1-F_h\left(\frac{s}{\mu}\right)\right]^{c}\right)^{R-1}\left[1-F_h\left(\frac{s}{\mu}\right)\right]^{c-1}\\ F_h\left(\frac{s}{\mu}\right)f_h\left(\frac{s}{\mu}\right)+\left(1-\left[1-F_h\left(\frac{s}{\mu}\right)\right]^{c}\right)^{R}f_h\left(\frac{s}{\mu}\right)\end{array}\right)\mathrm{d}s, \tag{10}$$

where $f_n(y)$ represents the PDF of AWGN, y_0 and y_1 denote no optical pulse and optical pulse, respectively, and $\otimes$ represents the convolution operation.

Normally, the fixed decision threshold (FDT) scheme refers to that all the detected signals are decided by using a fixed decision threshold y_{th}, satisfying $y_{\mathrm{th}}>0$. When the fixed decision threshold is given, the expressions of the probability of miss ($P_{\mathrm{m}}=\int_{-\infty}^{y_{\mathrm{th}}}f\left(y|\,y_1\right)\mathrm{d}y$) and false alarm ($P_{\mathrm{f}}=\int_{y_{\mathrm{th}}}^{\infty}f\left(y|\,y_0\right)\mathrm{d}y$) for the present communication system can be obtained. Assuming that every slot is independent, the *SER* is derived as

$$P_{\mathrm{S}}=1-P_{\mathrm{C}}=1-\left(1-P_{\mathrm{m}}\right)^{P}\left(1-P_{\mathrm{f}}\right)^{Q-P}=1-\frac{1}{2^{Q}}\times[1+$$
$$\mathrm{erf}\left(\frac{y_{\mathrm{th}}\sqrt{\overline{\gamma}}}{\mu}\right)]^{Q-P}[2-2\frac{\sqrt{\overline{\gamma}}}{\sqrt{\pi}}\exp\left(-\frac{\overline{\gamma}y_{\mathrm{th}}^2}{\mu^2}\right)\times$$
$$\int_0^\infty\exp\left(\frac{2y_{\mathrm{th}}\overline{\gamma}t}{\mu}\right)\exp\left(-\overline{\gamma}t^2\right)F_{\mathrm{M}}(t)\mathrm{d}t]^{P}, \tag{11}$$

where P_{C} represents the probability of correct demodulation, erf(*x*) denotes the error function, and $\overline{\gamma}=\mu^2/N_0$ is the average *SNR*. Moreover, performing the parameter change $x=\gamma t^2$ and with the help of generalized Gauss-Laguerre quadrature function[17], the *SER* expression for (*Q*, *P*) MPPM scheme of UWOC system with FDT scheme can be derived as

$$P_{\mathrm{S}}\approx1-\frac{1}{2^{Q}}\left(1+\mathrm{erf}\left(\frac{y_{\mathrm{th}}\sqrt{\overline{\gamma}}}{\mu}\right)\right)\times$$
$$[2-\frac{1}{\sqrt{\pi}}\exp\left(-\frac{\overline{\gamma}y_{\mathrm{th}}^2}{\mu^2}\right)\times$$
$$\sum_{i=0}^{n}H_i\exp\left(\frac{2y_{\mathrm{th}}\sqrt{\overline{\gamma}x_i}}{\mu}\right)\times F_{\mathrm{M}}\left(\sqrt{\frac{x_i}{\overline{\gamma}}}\right)]^{P}. \tag{12}$$

And with the increase of average *SNR* $\overline{\gamma}$, $\lim_{\overline{\gamma}\to\infty}P_{\mathrm{f}}=0$ and $\lim_{\overline{\gamma}\to\infty}P_{\mathrm{m}}=F_{\mathrm{M}}(\frac{y_{\mathrm{th}}}{\mu})$ can be got. Thus, the error floor for (*Q*, *P*) MPPM scheme of UWOC system with FDT scheme can be derived as

$$\lim_{\overline{\gamma}\to\infty}P_{\mathrm{S}}=1-\left(1-\lim_{\overline{\gamma}\to\infty}P_{\mathrm{m}}\right)^{P}=1-\left(1-F_{\mathrm{M}}\left(\frac{y_{\mathrm{th}}}{\mu}\right)\right)^{P}. \tag{13}$$

Considering that the scintillation effect is a slow fading process with a coherence time in the order of millisecond, the dynamic decision threshold (DDT) scheme is introduced to mitigate the scintillation in the present UWOC system. The signal intensity can be monitored further in advance for the DDT scheme. Therefore, the decision threshold[13] can be appropriately expressed as $y_{\mathrm{th}}=\frac{\mu}{2}+\frac{\mu}{2\overline{\gamma}}\ln\frac{Q-P}{P}$. And the conditional *SER* of each slot for DDT can be obtained as

$$SLER_{\mathrm{cond}}=\frac{P}{2Q}\mathrm{erfc}\left[\frac{\left(\mu-y_{\mathrm{th}}\right)}{\sqrt{2}\sigma_n}\right]+\frac{Q-P}{2Q}\mathrm{erfc}\left(\frac{y_{\mathrm{th}}}{\sqrt{2}\sigma_n}\right)=$$
$$\frac{P}{2Q}\mathrm{erfc}\left[\frac{\sqrt{\overline{\gamma}}}{2}\left(1-\frac{1}{\sqrt{\overline{\gamma}}}\ln\left(\frac{Q}{P}-1\right)\right)\right]+$$
$$\frac{Q-P}{2Q}\mathrm{erfc}\left[\frac{\sqrt{\overline{\gamma}}}{2}\left(1+\frac{1}{\sqrt{\overline{\gamma}}}\ln\left(\frac{Q}{P}-1\right)\right)\right], \tag{14}$$

where erfc(*x*) represents the complementary error function. Then, the *SER* of each slot affected by the absorption, scattering, ocean turbulence and misalignment effect of seawater can be expressed as $SLER=\int_0^\infty SLER_{\mathrm{cond}}f_{\mathrm{M}}(h)\mathrm{d}h$.

Therefore, the *SER* of the DDT scheme with (*Q*, *P*) MPPM in the present UWOC system can be denoted as

$$P_{\mathrm{S}}=1-(1-SLER)^{Q}=$$
$$1-(1-\int_0^\infty SLER_{\mathrm{cond}}f_{\mathrm{M}}(h)\mathrm{d}h)^{Q}. \tag{15}$$

Using integration by part with $\int w'v\mathrm{d}x = wv - \int wv'\mathrm{d}x$ for Eq.(15) and performing variable substitution $x = \overline{r}h^2/4$ and generalized Gauss-Laguerre quadrature function, the closed-form expression of *SER* for MPPM UWOC system with DDT scheme can be derived as

$$P_S = 1 - \{1 - \frac{P}{2\sqrt{\pi}Q}\sum_{i=1}^{n} H_i[\left(\frac{Q}{P}-1\right)^{\frac{1}{2}-\frac{\ln(Q/P-1)}{16x_i}} \times F_M\left(2\sqrt{\frac{x_i}{\overline{\gamma}}}\right) \times \left(1+\frac{\ln(Q/P-1)}{4x_i}\right)] - \frac{Q-P}{2\sqrt{\pi}Q}\sum_{i=1}^{n} H_i[\left(\frac{Q}{P}-1\right)^{-\frac{1}{2}-\frac{\ln(Q/P-1)}{16x_i}} \times F_M\left(2\sqrt{\frac{x_i}{\overline{\gamma}}}\right) \times \left(1-\frac{\ln(Q/P-1)}{4x_i}\right)]\}^Q. \quad (16)$$

The analytical results of the *SER* performance of the (5, 2) MPPM multi-hop parallel UWOC system with FDT and DDT schemes have been achieved from Eq.(12) and Eq.(16), respectively. Here, *N* is chosen to be 50 as computing the generalized Gauss-Laguerre approximations. The parameters adopted are given in Tab.2 and Tab.3[6]. Specifically, the acceptance/rejection method is used when generating the channel parameters of the mixture EGG distribution in the MC simulation. For the sake of generality, it is assumed that the distance in each link is the same, and the average transmission power on each node is equal. Furthermore, more than 10^8 random numbers are generated to reduce the statistical uncertainty in numerical simulations. And the computed PDF of the proposed UWOC system (one path and one hop) over composite EGG distributed channel has been compared with the measured data of the EGG channel[6] in Fig.2. It can be clearly seen in Fig.2 that the proposed composited EGG distributed channel quite matches the measured data.

Tab.2 Parameters of EGG distribution without salinity

BL (L/min)	Temperature gradient (°C/cm)	Parameters of EGG distribution ($\varpi, \lambda_{EGG}, a_{EGG}, b_{EGG}, c_{EGG}$)
2.4	0.05	0.213 0,0.329 1,1.429 9,1.181 7,17.198 4
2.4	0.10	0.210 8,0.269 4,0.602 0,1.279 5,21.161 1
2.4	0.15	0.180 7,0.164 1,0.233 4,1.420 1,22.592 4
2.4	0.20	0.166 5,0.120 7,0.155 9,1.521 6,22.875 4
4.7	0.05	0.458 9,0.344 9,1.042 1,1.576 8,35.942 4
4.7	0.10	0.453 9,0.274 4,0.300 8,1.705 3,54.142 2

Tab.3 Parameters of EGG distribution with salinity

Water type	*BL* (L/min)	Parameters of EGG distribution ($\varpi, \lambda_{EGG}, a_{EGG}, b_{EGG}, c_{EGG}$)
Salty	4.7	0.206 4,0.395 3,0.530 7,1.215 4,65.736 8
Salty	7.1	0.434 4,0.474 7,0.393 5,1.450 6,77.024 5
Fresh	4.7	0.210 9,0.460 3,1.252 6,1.150 1,41.325 8
Fresh	7.1	0.348 9,0.477 1,0.431 9,1.453 1,74.365 0

Fig.3 presents the *SER* performance of (5, 2) MPPM multi-hop parallel UWOC system with two hard decision schemes under three different water types. As can be seen, when using a fixed decision threshold, the *SER* will gradually approach a fixed value (the error floor) with the increase of the *SNR*. Meanwhile, the error floor will decrease with the reduction of the decision threshold y_{th} and the temperature gradient for three seawater types, as well as the lower concentration of dissolved particles. For example, in the clean ocean condition (c=0.151) and the temperature of 0.05 °C/cm in Fig.3(b), the error floors with *BL* of 4.7 L/min are about 7.5×10^{-3}, 1.9×10^{-4} and 8.0×10^{-6} for y_{th}=0.1μ, y_{th}=0.04μ and y_{th}=0.02μ, respectively. However, when coastal ocean (c=0.398) is considered, the corresponding error floors are approximately 1.6×10^{-2}, 5.1×10^{-4} and 2.4×10^{-5}, respectively. And compared with FDT scheme, obviously, DDT scheme not only eliminates the effect of the error floor but also has better *SER* performance.

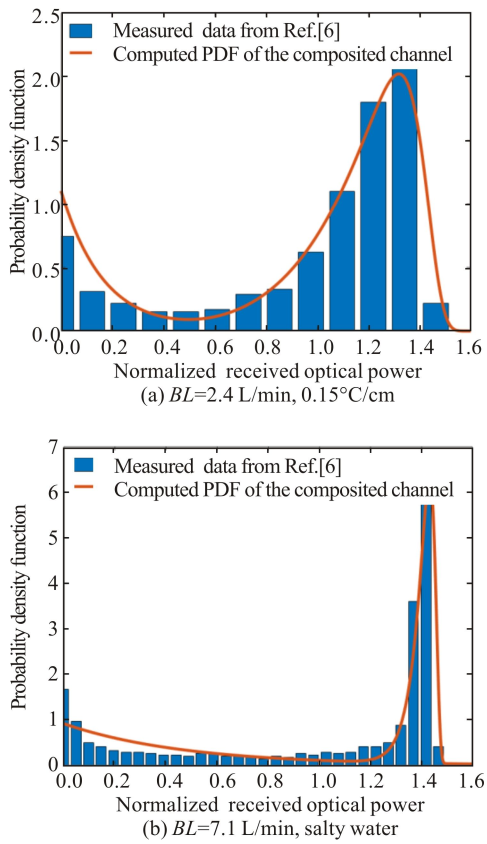

Fig.2 Histograms of the measured data along with the computed PDF over composite EGG distributed channel of the UWOC system (one path and one hop)

The *SER* performance of (5, 2) MPPM multi-hop parallel UWOC system with DDT scheme for different temperature gradients and *BLs* under three water types has been shown in Fig.4. It can be clearly observed that the temperature gradient affects the system performance obviously. Specifically, in the coastal ocean in Fig.4(c), at the given *SER* of 10^{-6}, when the temperature gradients are set to 0.05 °C/cm, 0.10 °C/cm, 0.15 °C/cm and 0.20 °C/cm, the corresponding *SNRs* of about 39.5 dB, 41 dB, 44 dB and 46 dB are required, respectively. And as can be observed, no matter what kind of seawater types, the *SER* performance deteriorates with the increase of *BLs*. For instance, under the condition of pure sea water (c=0.043) with the temperature gradient of 0.05 °C/cm in Fig.4(a), when the *SER* achieves 10^{-6}, the *SNR* required with *BL* of 2.4 L/min is about 36 dB, while the *SNR* required with *BL* of 4.7 L/min is about 43 dB. Furthermore, as can be observed in Fig.5, no matter what kind of seawater types, the *SER* performance deteriorates under the condition of salty water than fresh water. Specifically, under the condition of coastal ocean (c=0.398) in Fig.5(c) and at the given *SER* of 10^{-6}, when the *BL* is 4.7 L/min under the conditions of fresh water and salty water, the corresponding *SNRs* of about 36 dB and 37.5 dB are needed, respectively. When the *BL* is 7.1 L/min under the conditions of fresh water and salty water, the corresponding *SNRs* of about 41 dB and 43 dB are needed, respectively. This is mainly because that the oceanic turbulence would be stronger with the increase of the optical scintillation index (σ^2) caused by the raise of the temperature gradient, *BL* and water salinity, which therefore would lead to the *SER* deterioration of this UWOC system. And it can be clearly found in Fig.5 that the water salinity affects the system performance but in a much lesser degree than air bubbles, which cause rapid intensity fluctuations.

In addition, the increasing concentration of dissolved substances will also induce substantial deterioration of the system *SER* performance regardless of the temperature gradient or the *BL*. For instance, comparing (a), (b) and (c) in Fig.4, when the temperature gradient is 0.15 °C/cm with the *BL* of 2.7 L/min, and to achieve the *SER* of 10^{-6}, the corresponding *SNRs* required in the three seawater environments are approximately 41 dB, 42 dB and 44 dB, respectively. And as can be found, when the *BL* is 4.7 L/min with temperature gradient of 0.05 °C/cm, and at the given *SER* of 10^{-6}, the corresponding *SNRs* of about 43 dB, 44 dB and 46.5 dB are needed for these three seawater environments, respectively. And as can be found in Fig.5, when the *BL* is 7.1 L/min with salty water, and at the given *SER* of 10^{-6}, the corresponding *SNRs* of about 40 dB, 41 dB and 43 dB are needed for these three seawater environments, respectively.

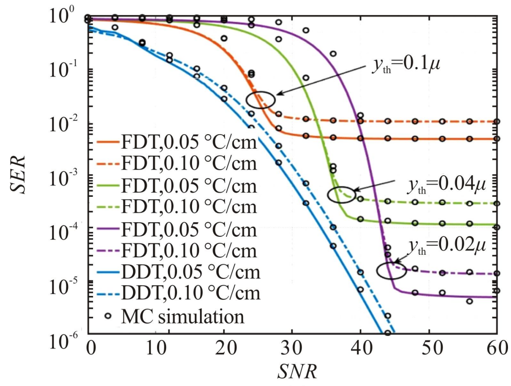

(a)

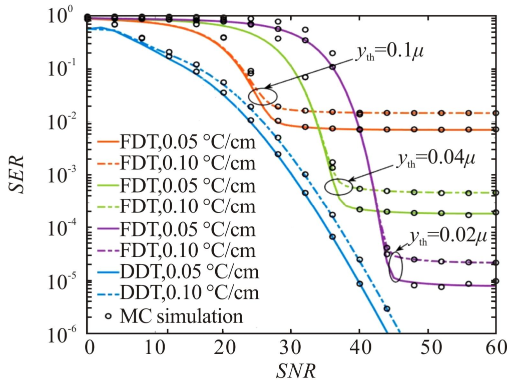

(b)

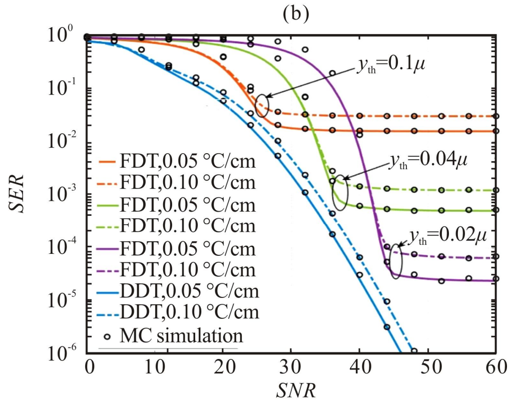

(c)

Fig.3 *SER* performance of (5, 2) MPPM multi-hop parallel UWOC system (*R*=4, *C*=3) with two different schemes under three water types (*BL*=4.7 L/min): (a) Pure sea water; (b) Clean ocean; (c) Coastal ocean

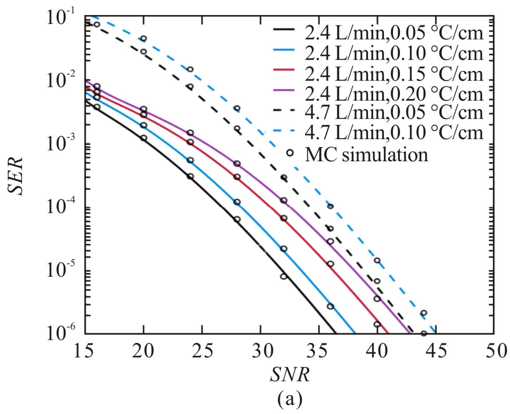

(a)

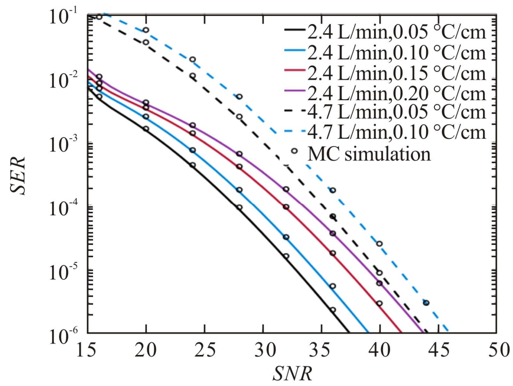

(b)

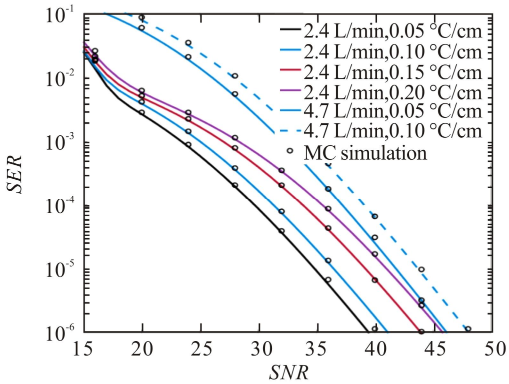

(c)

Fig.4 *SER* performance of (5, 2) MPPM multi-hop parallel UWOC system (*R*=4, *C*=3) with DDT scheme for different temperature gradients and *BLs* under three water types: (a) Pure sea water; (b) Clean ocean; (c) Coastal ocean

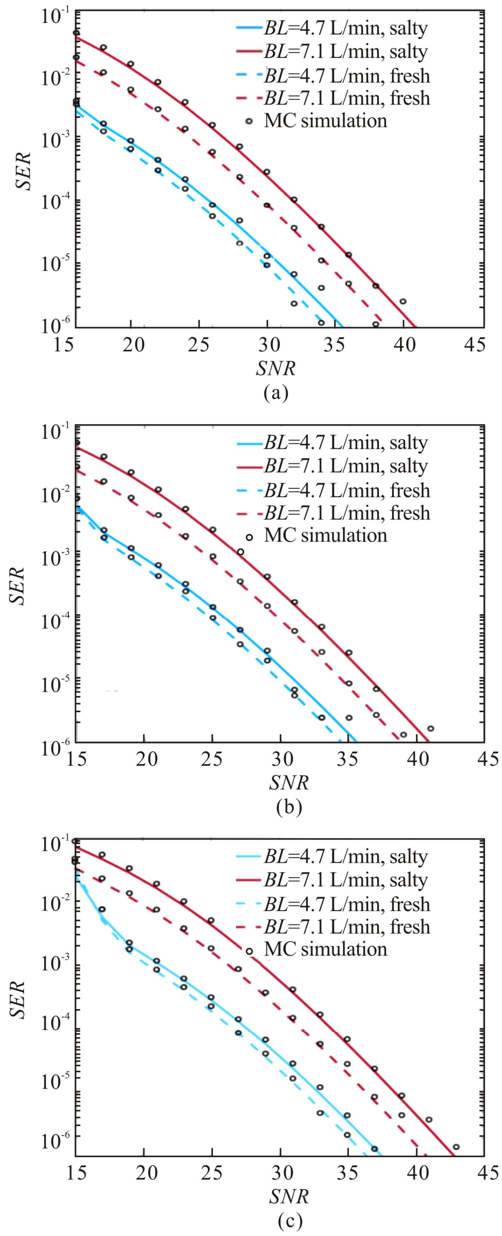

Fig.5 *SER* performance of (5, 2) MPPM multi-hop parallel UWOC system (*R*=4, *C*=3) with DDT scheme considering water gradient under three water types: (a) Pure sea water; (b) Clean ocean; (c) Coastal ocean

Fig.6(a) demonstrates the *SER* performance of the present UWOC system using DDT scheme with different numbers of parallel paths. As shown in the figure, the *SER* performance can be improved by increasing the number of cooperative paths (*R*). Increasing *R* from 1 to 4, an *SER* performance gain of approximately 12.5 dB could be got for a given *SER* of 10^{-6}. This is because the influence of optical absorption, scattering, ocean turbulence and misalignment loss would be weakened with the increase of parallel paths in seawater, and thus the performance of the present UWOC system would be improved. Fig.6(b) gives the *SER* performance with DDT scheme under different hop counts. As can be seen, with the increasing hop counts, the system performance will suffer a certain deterioration. However, with the increasing *C*, the total link distance of the system transmission will be expanded.

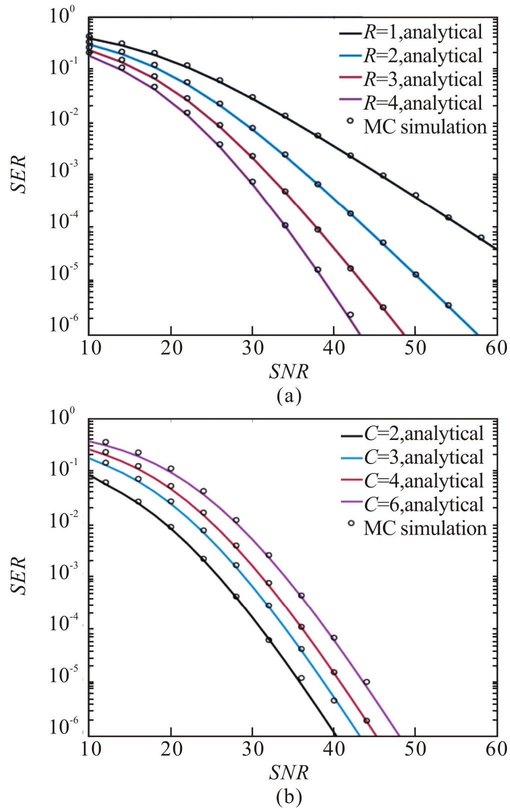

Fig.6 *SER* performance of the multi-hop parallel UWOC system with DDT scheme with different structure parameters (*BL*=4.7 L/min, 0.05 °C/min): (a) Different numbers of cooperative paths (*R*=1, 2, 3, 4, *C*=3); (b) Different hop counts (*R*= 4, *C*=2, 3, 4, 6)

In this work, on the basis of the aggregated EGG oceanic turbulence fading model combining the impacts of absorption, scattering and misalignment loss characterized by BSF, the *SER* performance of a multi-hop parallel UWOC system with MPPM scheme has been investigated involving two different hard decision schemes.

With the help of Gauss-Laguerre quadrature function, the theoretical *SER* expressions for hard decision demodulation of FDT and DDT schemes are derived respectively, which are verified by MC simulations. Furthermore, the impacts of different *BLs*, temperature gradients and water salinity on the *SER* performance are studied for different water types and structure parameters. Results show that the UWOC system with DDT scheme could overcome the error floor caused by FDT scheme, and it has better system performance than that with FDT scheme under the same conditions. This study also indicates that the raise of optical scintillation index is introduced by high temperature gradient, *BL* and water salinity. And the increasing concentration of dissolved particles in the seawater environment would induce the deterioration of system performance. Furthermore, multi-hop parallel transmission could effectively improve the UWOC system performance. The above results are helpful for the design and development of the relay-assisted UWOC system.

Statements and Declarations

The authors declare that there are no conflicts of interest related to this article.

References

[1] JIANG H, QIU H, HE N, et al. Ergodic capacity and error performance of spatial diversity UWOC systems over generalized gamma turbulence channels[J]. Optics communications, 2022, 505：127476.

[2] KODAMA T, SANUSI M A B A, KOBORI F, et al. Comprehensive analysis of time-domain hybrid PAM for data-rate and distance adaptive UWOC system[J]. IEEE access, 2021, 9：57064-57074.

[3] KUMAR L B, KRISHNAN P. Multi-hop convergent FSO-UWOC system to establish a reliable communication link between the islands[J]. Optics communications, 2020, 474：126107-126113.

[4] YANG L, ZHU Q, LI S, et al. On the performance of mixed FSO-UWOC dual-hop transmission systems[J]. IEEE wireless communications letters, 2021, 10(9)：2041-2045.

[5] LU H, JIANG M, CHENG J. Deep learning aided robust joint channel classification, channel estimation, and signal detection for underwater optical communication[J]. IEEE transactions on communications, 2021, 69(4)：2290-2303.

[6] ZEDINI E, OUBEI H M, KAMMOUN A, et al. Unified statistical channel model for turbulence-induced fading in underwater wireless optical communication systems[J]. IEEE transactions on communications, 2019, 67(4)：2893-2907.

[7] PHOOKANO P P, ANEES S. Performance analysis of distributed alamouti based UWOC system[C]//3rd International Conference on Advanced Communication Technologies and Networking, CommNet 2020, September 4-6, 2020, Marrakech, Morocco. New York：IEEE, 2020：1-5.

[8] LEI H, ZHANG Y, PARK K H, et al. Performance analysis of dual-hop RF-UWOC systems[J]. IEEE photonics journal, 2020, 12(2)：1-15.

[9] LI S, WANG P, PANG W, et al. Performance analysis for cooperative communication system in optical IoUT network with HDAF strategy[J]. IEEE photonics journal, 2021, 13(3)：1-22.

[10] SAXENA P, BHATNAGAR M R. A simplified form of beam spread function in underwater wireless optical communication and its applications[J]. IEEE access, 2019, 7：105298-105313.

[11] LI A, WANG P, PANG W, et al. ABER performance investigation of LDPC-coded multi-hop parallel underwater wireless optical communication system[J]. Applied optics, 2020, 59(5)：1353-1362.

[12] BYKHOVSKY D, ARNON S. Performance of spectral amplitude coded multiple pulse position modulation with non-uniform energy slots and fading[J]. Optics express, 2018, 26(22)：29225-29230.

[13] QIN Y, WANG P, LIU X, et al. Optical communication system with two decision thresholds over exponentiated Weibull fading channels[J]. Optics communications, 2018, 424：91-97.

[14] DU Y, LI S, WANG P, et al. Performance analysis of multi-hop underwater wireless optical communication system with space-time block codes considering the impact of beam spread function[J]. Optical engineering, 2022, 61(3)：15602303.

[15] PAN Y, WANG P, WANG W, et al. Statistical model for the weak turbulence-induced attenuation and crosstalk in free space communication systems with orbital angular momentum[J]. Optics express, 2021, 29(8)：12644-12662.

[16] DONG Y, TANG S, ZHANG X. Effect of random sea surface on downlink underwater wireless optical communications[J]. IEEE communications letters, 2013, 17(11)：2164-2167.

[17] CONCUS P, CASSATT D, JAEHNIG G, et al. Tables for the evaluation of $\int_0^\infty x^\beta e^{-x} f(x)dx$ by Gauss-Laguerre quadrature[J]. Mathematics of computation, 1963, 17：245.